Strange nucleon form factors in the perturbative chiral quark model

V. E. Lyubovitskij, P. Wang, Th. Gutsche, and Amand Faessler
Institut für Theoretische Physik, Universität Tübingen, Auf der Morgenstelle 14, D-72076 Tübingen, Germany
(Received 19 July 2002; published 6 November 2002)

We apply the perturbative chiral quark model at one loop to calculate the strange form factors of the nucleon. A detailed numerical analysis of the strange magnetic moments and radii of the nucleon, and also the momentum dependence of the form factors is presented.

DOI: 10.1103/PhysRevC.66.055204 PACS number(s): 12.39.Fe, 12.39.Ki, 13.40.Gp, 14.20.Dh

I. INTRODUCTION

Strange quark contributions to the properties of the nucleon have attracted a lot of interest since the originally puzzling EMC results of the proton spin [1]. Recently, the SAMPLE [2,3] and HAPPEX [4,5] Collaborations reported results for the strange nucleon form factors from the measurement of the parity-violating asymmetry in elastic electron-proton scattering. The SAMPLE Collaboration at MIT-Bates [2,3] concentrated on the strange magnetic form factor G_M^s at a small momentum transfer with $Q_S^2 = 0.1$ GeV^2. The updated value of G_M^s measured by the SAMPLE Collaboration [3] is

$$G^s_{\rm SAMPLE}(Q^2_{\rm S}) \doteq G^s_M(Q^2_{\rm S}) = 0.14 \pm 0.29 \pm 0.31. \tag{1}$$

Here and in the following, results for the magnetic form factor are given in units of nuclear magnetons. The HAPPEX Collaboration at TJNAF [4,5] extracted from the data the combination of charge G_E^s and magnetic G_M^s form factor

$$\begin{aligned} G^s_{\rm HAPPEX}(Q^2_{\rm H}) &\doteq G^s_E(Q^2_{\rm H}) + 0.39 G^s_M(Q^2_{\rm H}) \\ &= 0.025 \pm 0.020 \pm 0.014 \end{aligned} \tag{2}$$

at $Q^2_{\rm H} = 0.477$ GeV^2 [5]. The upcoming experiment by the A4 Collaboration at MAMI [6] intends to measure

$$G^s_{\rm MAMI}(Q^2_{\rm M}) \doteq G^s_E(Q^2_{\rm M}) + 0.22 G^s_M(Q^2_{\rm M}), \tag{3}$$

where $Q^2_{\rm M} = 0.23$ GeV^2.

Different theoretical approaches were applied to the analysis of strange nucleon form factors, including QCD equalities and Lattice QCD [7–10], heavy baryon chiral perturbation theory (HBChPT) [11,12], dispersive approaches [13–15], kaon loop calculations [16], a hybrid model based on vector meson dominance (VMD) in addition to a kaon cloud contribution [17], a VMD model [18], a Skyrme model [19], a NJL model [20], and chiral [21] soliton models, chiral bag [22] and chiral quark [23,24] models, etc. Theoretical results vary quite widely. For example, the predictions for the strange magnetic moment $\mu_N^s \doteq G_M^S(0)$ are distributed from negative values -0.75 ± 0.30 [7] to positive ones 0.37 [22]. Theoretical results for the strange charge radius vary from -0.16 ± 0.06 fm^2 [9] to 0.05 ± 0.09 fm^2 [12]. Similarly, predictions for the momentum dependence of the strange form factors cover a wide range of values, depending on the individual model. Therefore, more precise experiments can serve as a crucial check for existing low-energy approaches, which describe the sea of strange quarks inside the nucleon.

Here we concentrate on the calculation of the strange nucleon form factors in the framework of the perturbative chiral quark model (PCQM) which was suggested and developed in Refs. [25–28] for the study of low-energy properties of baryons. The PCQM is based on the nonlinear σ-model quark Lagrangian, and includes a phenomenological confinement potential. Baryons are considered as bound states of valence quarks surrounded by a cloud of pseudoscalar mesons. We treat the meson cloud perturbatively and, therefore, our approach is similar to quark models studied in Refs. [24,29–31]. The model was successfully applied to the electromagnetic properties of the nucleon [26], σ-term physics [27], and the πN scattering including radiative corrections [28].

In the present paper we proceed as follows. In Sec. II we briefly describe the basic notions of our approach. In Sec. III we apply the model to investigate the strange form factors of nucleon. Section IV contains a summary of our major conclusions.

II. PERTURBATIVE CHIRAL QUARK MODEL

The starting point of the perturbative chiral quark model [26–28] is an effective chiral Lagrangian describing the valence quarks of baryons as relativistic fermions moving in a self-consistent field (static potential) $V_{\rm eff}(r) = S(r) + \gamma^0 V(r)$ with $r = |\vec{x}|$ [25,30], which are supplemented by a cloud of Goldstone bosons (π, K, η). (For details, see Ref. [26].) The effective Lagrangian $\mathcal{L}_{\rm eff} = \mathcal{L}_{\rm inv} + \mathcal{L}_{\chi SB}$ of the PCQM includes a chiral invariant part $\mathcal{L}_{\rm inv}$ and a symmetry breaking term $\mathcal{L}_{\chi SB}$ (containing the mass terms for quarks and mesons),

$$\begin{aligned} \mathcal{L}_{\rm inv}(x) &= \bar{\psi}(x)[i\not{\partial} - \gamma^0 V(r)]\psi(x) + \frac{1}{2}[D_\mu \Phi_i(x)]^2 \\ &\quad - S(r)\bar{\psi}(x)\exp\left[i\gamma^5 \frac{\hat{\Phi}(x)}{F}\right]\psi(x), \end{aligned} \tag{4}$$

$$\mathcal{L}_{\chi SB}(x) = -\bar{\psi}(x)\mathcal{M}\psi(x) - \frac{B}{2}{\rm Tr}[\hat{\Phi}^2(x)\mathcal{M}], \tag{5}$$

where $\hat{\Phi}(x)$ is the octet matrix of pseudoscalar mesons, D_μ is the covariant derivative [27], $F=88$ MeV [26,32] is the pion decay constant in the chiral limit, $\mathcal{M}=\mathrm{diag}\{\hat{m},\hat{m},m_s\}$ is the mass matrix of current quarks with $\hat{m}=7$ MeV, and $m_s=25\hat{m}$; $B=1.4$ GeV is the quark condensate constant. (Here we restrict ourselves to the isospin symmetry limit with $m_u=m_d=\hat{m}$.) We rely on the standard picture of chiral symmetry breaking [33] and for the masses of pseudoscalar mesons we use the leading term in their chiral expansion (i.e., linear in the current quark mass):

$$M_\pi^2=2\hat{m}B, \quad M_K^2=(\hat{m}+m_s)B, \quad M_\eta^2=\frac{2}{3}(\hat{m}+2m_s)B. \tag{6}$$

We expand the quark field ψ in the basis of potential eigenstates as

$$\psi(x)=\sum_\alpha b_\alpha u_\alpha(\vec{x})\exp(-i\mathcal{E}_\alpha t)+\sum_\beta d_\beta^\dagger v_\beta(\vec{x})\exp(i\mathcal{E}_\beta t), \tag{7}$$

where the sets of quark $\{u_\alpha\}$ and antiquark $\{v_\beta\}$ wave functions in orbits α and β are solutions of the Dirac equation with the static potential. The expansion coefficients b_α and $d_\beta^\dagger$ are the corresponding single quark annihilation and antiquark creation operators.

Treating Goldstone fields as small fluctuations around the three-quark $(3q)$ core we formulate perturbation theory in the expansion parameter $\hat{\Phi}(x)/F\sim 1/\sqrt{N_c}$ which corresponds to an expansion in powers of p/F, where p is the 3 momentum of the meson field. We also treat finite current quark masses perturbatively [26,33]. In this paper we restrict ourselves to the linear form of the meson-quark interaction $\exp[i\gamma^5\hat{\Phi}(x)/F]\approx 1+i\gamma^5\hat{\Phi}(x)/F$, and all calculations are performed at one loop or at order of accuracy $o(1/F^2,\hat{m},m_s)$. In the calculation of matrix elements we project quark diagrams on the respective baryon states. The baryon states are conventionally set up by the product of the SU(6) spin-flavor and $\mathrm{SU}(3)_c$ color wave functions, where the nonrelativistic single quark spin wave function is replaced by the relativistic solution $u_\alpha(\vec{x})$ of the Dirac equation

$$[-i\gamma^0\vec{\gamma}\cdot\vec{\nabla}+\gamma^0 S(r)+V(r)-\mathcal{E}_\alpha]u_\alpha(\vec{x})=0, \tag{8}$$

where $\mathcal{E}_\alpha$ is the single-quark energy.

For the description of baryon properties we use the effective potential $V_{\mathrm{eff}}(r)$ with quadratic radial dependencies [26,27]

$$S(r)=M_1+c_1 r^2, \quad V(r)=M_2+c_2 r^2 \tag{9}$$

with the particular choices

$$M_1=\frac{1-3\rho^2}{2\rho R}, \quad M_2=\mathcal{E}_0-\frac{1+3\rho^2}{2\rho R}, \quad c_1\equiv c_2=\frac{\rho}{2R^3}. \tag{10}$$

Here $\mathcal{E}_0$ is the single-quark ground-state energy; R are ρ are parameters related to the ground-state quark wave function u_0,

$$u_0(\vec{x})=N\exp\left[-\frac{\vec{x}^2}{2R^2}\right]\begin{pmatrix}1\\ i\rho\vec{\sigma}\vec{x}/R\end{pmatrix}\chi_s\chi_f\chi_c, \tag{11}$$

where $N=[\pi^{3/2}R^3(1+3\rho^2/2)]^{-1/2}$ is a normalization constant; χ_s, χ_f, and χ_c are the spin, flavor and color quark wave functions, respectively. Note that the constant part of the scalar potential M_1 can be interpreted as the constituent mass of the quark, which is simply the displacement of the current quark mass due to the potential $S(r)$. The parameter ρ is related to the axial charge g_A of the nucleon calculated in zeroth-order (or $3q$-core) approximation:

$$g_A=\frac{5}{3}\left(1-\frac{2\rho^2}{1+\frac{3}{2}\rho^2}\right). \tag{12}$$

Therefore, ρ can be replaced by g_A using matching condition (12). The parameter R is related to the charge radius of the proton in the zeroth-order approximation as

$$\langle r_E^2\rangle_{LO}^P=\int d^3x u_0^\dagger(\vec{x})\vec{x}^2 u_0(\vec{x})=\frac{3R^2}{2}\frac{1+\frac{5}{2}\rho^2}{1+\frac{3}{2}\rho^2}. \tag{13}$$

In our calculations we use the value $g_A=1.25$ [26]. Therefore, we have only one free parameter, that is R. In the numerical studies [26] R is varied in the region from 0.55 to 0.65 fm, which corresponds to a change of $\langle r_E^2\rangle_{LO}^P$ from 0.5 to 0.7 fm^2. The parameter R serves as a scale parameter for perturbation theory. In a previous paper [26] we showed that for values of $R=0.6\pm 0.05$ fm our perturbation theory is perfectly justified. We calculated the renormalization constant Z which is responsible for charge conservation. The numerical value of Z for our set of parameters is close to unity (e.g., for nonstrange quarks 0.88 ± 0.03). The expansion $\hat{\phi}/F$ breaks down for $R<0.3$ fm. With the formal and phenomenological foundation established, our model gives a reasonable description of nucleon properties. In models similar to our approach (see, e.g., Ref. [34]) an improvement of the phenomenological fit can be obtained by inclusion of certain additional physical aspects, such as c.m. corrections and Lorentz boost effects. Usually, these two types of corrections are calculated for leading (three-quark core) diagrams [34] while their contributions are supposed to be negligible for next-to-leading diagrams including meson cloud corrections. The contributions to the strange nucleon form factors start with next-to-leading diagrams. Therefore, we do not include center-of-mass and Lorentz boosts corrections. In our further publications we intend to calculate these effects.

III. STRANGE FORM FACTORS OF NUCLEON

Now we consider the calculation of the strange vector and axial vector nucleon form factors. We first derive from the model Lagrangian the strangeness vector current $V_\mu^{\rm s}$, which is the combination of the baryonic $J_\mu^{\rm B}$ and the hypercharge $J_\mu^{\rm Y}$ currents:

$$V_\mu^{\rm s} \doteq J_\mu^{\rm B} - J_\mu^{\rm Y}. \tag{14}$$

Using Noether's theorem we have

$$J_\mu^{\rm B} = \frac{1}{3}\bar{q}\gamma_\mu q, \quad J_\mu^{\rm Y} = \bar{q}\gamma_\mu \frac{\lambda_8}{\sqrt{3}} q + \frac{2}{\sqrt{3}} f_{8ij}\Phi_i \partial_\mu \Phi_j, \tag{15}$$

where f_{ijk} are the totally antisymmetric structure constants of SU(3). We therefore obtain

$$V_\mu^{\rm s} = \bar{s}\gamma_\mu s + (K^+ i\partial_\mu K^- + K^0 i\partial_\mu \bar{K}^0 + \text{H.c.}). \tag{16}$$

Note that both valence and sea (K-meson cloud) quarks contribute to the strangeness vector current. This form of the strangeness current is common to chiral quark models [24]. The strangeness axial current $A_\mu^{\rm s}$ is given by

$$A_\mu^{\rm s} = \bar{s}\gamma_\mu\gamma_5 s, \tag{17}$$

where, because of the pseudoscalar nature of the Goldstone bosons, the mesonic piece is absent. To perform a consistent calculation of strange nucleon form factors we have to guarantee local gauge invariance associated with the electromagnetic $U_{\rm em}(1)$ group. As in the case of electromagnetic form factors (see Ref. [26]), we restrict our kinematics to a specific frame, that is the Breit frame (BF), where gauge invariance is fulfilled due to the decoupling of the time and vector components of the electromagnetic current operator [35]. In the BF the initial momentum of the nucleon is $p = (E, -\vec{q}/2)$, the final momentum is $p' = (E, \vec{q}/2)$ and the 4-momentum-transfer is $q = (0, \vec{q})$ with $p' = p + q$. With the spacelike momentum transfer squared given as $Q^2 = -q^2 = \vec{q}^{\,2}$, the strange form factors of nucleon—charge $G_E^{\rm s}$ and magnetic $G_M^{\rm s}$ (Sachs) form factors—are defined in the BF by

$$\left\langle N\left(\frac{\vec{q}}{2}\right)\middle| V_0^{\rm s}(0) \middle| N\left(-\frac{\vec{q}}{2}\right)\right\rangle = \chi_N^\dagger \chi_N G_E^{\rm s}(Q^2), \tag{18}$$

$$\left\langle N\left(\frac{\vec{q}}{2}\right)\middle| \vec{V}^{\rm s}(0) \middle| N\left(-\frac{\vec{q}}{2}\right)\right\rangle = \chi_N^\dagger \frac{i\vec{\sigma}_N \times \vec{q}}{2m_N} \chi_N G_M^{\rm s}(Q^2), \tag{19}$$

$$\left\langle N\left(\frac{\vec{q}}{2}\right)\middle| A_3^{\rm s}(0) \middle| N\left(-\frac{\vec{q}}{2}\right)\right\rangle = \chi_N^\dagger \sigma_N^3 \chi_N G_A^{\rm s}(Q^2). \tag{20}$$

Here, $V_0^{\rm s}$ and $\vec{V}^{\rm s}$ are the time and space component of the strangeness vector current [Eq. (16)] $A_3^{\rm s}$ is the third spatial component of the strangeness axial current [Eq. (17)]; χ_N is the nucleon spin wave function. At zero recoil the Sachs form factors satisfy the normalization conditions

$$G_E^{\rm s}(0) = 0, \quad G_M^{\rm s}(0) = \mu^{\rm s}, \quad G_A^{\rm s}(0) = g_A^{\rm s}, \tag{21}$$

where $\mu^{\rm s}$ and $g_A^{\rm s}$ are the strange nucleon magnetic moment and axial charge, respectively. Dirac $F_1^{\rm s}(Q^2)$ and Pauli $F_2^{\rm s}(Q^2)$ form factors are related to the Sachs form factors by

$$G_E^{\rm s}(Q^2) = F_1^{\rm s}(Q^2) - \frac{Q^2}{4m_N^2} F_2^{\rm s}(Q^2), \tag{22}$$

$$G_M^{\rm s}(Q^2) = F_1^{\rm s}(Q^2) + F_2^{\rm s}(Q^2). \tag{23}$$

The strange nucleon radii (charge, magnetic and axial) are given by

$$\langle r^2\rangle_{\rm I}^{\rm s} = -6\frac{dG_{\rm I}^{\rm s}(Q^2)}{dQ^2}\Big|_{Q^2=0}, \quad {\rm I} = E, M, A. \tag{24}$$

In the PCQM the strange vector (charge and magnetic) and axial form factors of the nucleon are defined by

$$\chi_N^\dagger \chi_N G_E^{\rm s}(Q^2) = {}^N\langle \phi_0 | -\frac{1}{2}\int \delta(t) d^4x d^4x_1 d^4x_2 e^{-iqx} \times T[\mathcal{L}_{int}(x_1)\mathcal{L}_{int}(x_2) V_0^{\rm s}(x)] |\phi_0\rangle_c^N, \tag{25}$$

$$\chi_N^\dagger \frac{i\vec{\sigma}_N \times \vec{q}}{2m_N}\chi_N G_M^{\rm s}(Q^2) = {}^N\langle \phi_0 | -\frac{1}{2}\int \delta(t) d^4x d^4x_1 d^4x_2 e^{-iqx} \times T[\mathcal{L}_{int}(x_1)\mathcal{L}_{int}(x_2) \vec{V}^{\rm s}(x)] |\phi_0\rangle_c^N, \tag{26}$$

$$\chi_N^\dagger \sigma_N^3 \chi_N G_A^{\rm s}(Q^2) = {}^N\langle \phi_0 | -\frac{1}{2}\int \delta(t) d^4x d^4x_1 d^4x_2 e^{-iqx} \times T[\mathcal{L}_{int}(x_1)\mathcal{L}_{int}(x_2) A_3^{\rm s}(x)] |\phi_0\rangle_c^N, \tag{27}$$

where $\mathcal{L}_{int}$ is the linearized strong interaction Lagrangian of kaons and quarks:

$$\mathcal{L}_{int}(x) = -\frac{S(r)}{F}[K^+(x)\bar{u}(x) i\gamma^5 s(x) + K^0(x)\bar{d}(x) i\gamma^5 s(x)] + \text{H.c.} \tag{28}$$

Superscript "N" in Eqs. (25) and (26) indicates that the matrix elements are projected on the respective nucleon states and subscript "c" refers to contributions from connected graphs only. At one loop the relevant diagrams are indicated by Figs. 1(a) (meson-cloud) and 1(b) (vertex correction). For the quark field we use a Feynman propagator for a fermion in a binding potential:

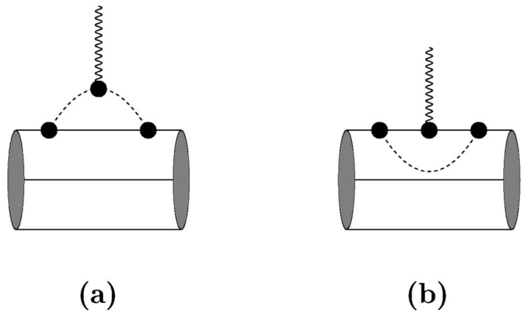

FIG. 1. Diagrams contribution to the strange nucleon form factors: (a) meson cloud diagram and (b) vertex correction diagram.

$$iG_\psi(x,y)=\theta(x_0-y_0)\sum_\alpha u_\alpha(\vec{x})\overline{u}_\alpha(\vec{y})e^{-i\mathcal{E}_\alpha(x_0-y_0)} - \theta(y_0-x_0)\sum_\beta v_\beta(\vec{x})\overline{v}_\beta(\vec{y})e^{i\mathcal{E}_\beta(x_0-y_0)}. \tag{29}$$

In the following we truncate the expansion of the quark propagator to the ground state eigenmode:

$$iG_\psi(x,y)\to iG_0(x,y)\doteq u_0(\vec{x})\overline{u}_0(\vec{y})e^{-i\mathcal{E}_\alpha(x_0-y_0)}\theta(x_0-y_0). \tag{30}$$

For K mesons we use the free Feynman propagator for a boson field with

$$i\Delta_K(x-y)=\int\frac{d^4k}{(2\pi)^4 i}\frac{\exp[-ik(x-y)]}{M_K^2-k^2-i\epsilon}. \tag{31}$$

Below, for transparency, we present the analytical expressions for the strange nucleon form factors obtained in the PCQM.

(a) The meson-cloud (MC) diagram [Fig. 1(a)] results in

$$G_E^s(Q^2)|_{MC}=-\frac{27}{200}\left(\frac{g_A}{\pi F}\right)^2\int_0^\infty dp\,p^2\int_{-1}^1 dx(p^2+p\sqrt{Q^2}x) \times\mathcal{F}_{\pi NN}(p^2,Q^2,x)t_E^{MC}(p^2,Q^2,x), \tag{32}$$

$$G_M^s(Q^2)|_{MC}=-\frac{9}{200}m_N\left(\frac{g_A}{\pi F}\right)^2\int_0^\infty dp\,p^4\int_{-1}^1 dx \times(1-x^2)\mathcal{F}_{\pi NN}(p^2,Q^2,x)t_M^{MC}(p^2,Q^2,x), \tag{33}$$

where

$$\mathcal{F}_{\pi NN}(p^2,Q^2,x)=F_{\pi NN}(p^2)F_{\pi NN}(p^2+\Delta),$$

$$\Delta=Q^2+2p\sqrt{Q^2}x,$$

$$t_E^{MC}(p^2,Q^2,x) =\frac{1}{w_K(p^2)w_K(p^2+\Delta)[w_K(p^2)+w_K(p^2+\Delta)]},$$

$$t_M^{MC}(p^2,Q^2,x)=\frac{1}{w_K^2(p^2)w_K^2(p^2+\Delta)}, \tag{34}$$

with $\omega_K(t)=\sqrt{M_K^2+t}$. Here $F_{\pi NN}(p^2)$ is the πNN form factor normalized to unity at zero recoil. For the *Gaussian* form of the single-quark wave function it is given by [26]

$$F_{\pi NN}(p^2)=\exp\left(-\frac{p^2R^2}{4}\right)\left\{1+\frac{p^2R^2}{8}\left(1-\frac{5}{3g_A}\right)\right\}. \tag{35}$$

(b) The vertex-correction (VC) diagram [Fig. 1(b)] contributes.

$$G_{E(M)}^s(Q^2)|_{VC}=G_{E(M)}^p(Q^2)|_{3q}^{LO}\frac{3}{200}\left(\frac{g_A}{\pi F}\right)^2 \times\int_0^\infty dp\,p^4\frac{F_{\pi NN}^2(p^2)}{w_K^3(p^2)}\cdot t_{E(M)}^{VC}, \tag{36}$$

$$G_A^s(Q^2)\equiv G_A^s(Q^2)|_{VC} =-G_A(Q^2)\,\frac{9}{1000}\left(\frac{g_A}{\pi F}\right)^2\int_0^\infty dp\,p^4\frac{F_{\pi NN}^2(p^2)}{w_K^3(p^2)}, \tag{37}$$

where $t_E^{VC}=9$ and $t_M^{VC}=-1$; $G_A(Q^2)=g_AF_{\pi NN}(Q^2)$ is the axial nucleon form factor; $G_{E(M)}^p(Q^2)|_{3q}^{LO}$ are the proton charge and magnetic form factors calculated at leading order (LO) [26]:

$$G_E^p(Q^2)|_{3q}^{LO}=\exp\left(-\frac{Q^2R^2}{4}\right)\left(1-\frac{\rho^2}{1+\frac{3}{2}\rho^2}\frac{Q^2R^2}{4}\right), \tag{38}$$

$$G_M^p(Q^2)|_{3q}^{LO}=\exp\left(-\frac{Q^2R^2}{4}\right)\frac{2m_N\rho R}{1+\frac{3}{2}\rho^2}. \tag{39}$$

For the case of the strange axial nucleon form factor only the VC diagram [Fig. 1(b)] contributes at the order of accuracy we are working in. Combining the contributions of both diagrams, the expressions for the static characteristics (the strange magnetic moments, radii and axial charge of the nucleon) are given by

TABLE I. Static strange characteristics associated with the vector current.

Approach	μ^s (n.m.)	$\langle r^2\rangle^s_E$ (fm^2)	$\langle r^2\rangle^s_M$ (fm^2)	ρ^s	$\rho^s+\mu_p\mu^s$
QCD equalities [7]	-0.75 ± 0.30				
Lattice QCD [8]	-0.16 ± 0.18				
Lattice QCD [9]	-0.36 ± 0.20	-0.16 ± 0.06		2.02 ± 0.75	1 ± 0.75
Lattice QCD [10]	-0.28 ± 0.10				
HBChPT [12]	0.18 ± 0.34	0.05 ± 0.09	-0.14		
Poles [13]	-0.31 ± 0.09	0.14 ± 0.07		-2.1	-2.97
Poles [14]	-0.185 ± 0.075	0.14 ± 0.06		-2.93	-3.60
Poles [15]	-0.24 ± 0.03				
Kaon loop [16]	-0.355 ± 0.045	-0.0297 ± 0.0026			
Kaon loop+VMD [17]	-0.28 ± 0.04	-0.0425 ± 0.0026			
Skyrme model [19]	-0.13	-0.11		1.64	1.27
NJL soliton model [20]	0.10 ± 0.15	-0.15 ± 0.05		3.06	2.92
χQSM [21]	0.115	-0.095	0.073		
CBM [22]	0.37				
CQM [23]	~-0.05				
CQM [24]	-0.046		~0.02		
PCQM	-0.048 ± 0.012	-0.011 ± 0.003	-0.024 ± 0.003	0.17 ± 0.04	0.05

$$\mu^s=-\frac{3}{200}\left(\frac{g_A}{\pi F}\right)^2\int_0^\infty \frac{dp\,p^4}{w_K^3(p^2)}F^2_{\pi NN}(p^2)\left[\mu_p^{LO}+\frac{4m_N}{w_K(p^2)}\right], \tag{40}$$

$$g_A^s=-\frac{9}{1000}\,g_A\left(\frac{g_A}{\pi F}\right)^2\int_0^\infty \frac{dp\,p^4}{w_K^3(p^2)}F^2_{\pi NN}(p^2), \tag{41}$$

$$\langle r^2\rangle^s_E=\frac{27}{200}\left(\frac{g_A}{\pi F}\right)^2\int_0^\infty\frac{dp\,p^4}{w_K^3(p^2)}\Bigg[F^2_{\pi NN}(p^2)\Bigg(\langle r_E^2\rangle^P_{LO}-\frac{5}{2}\,\frac{p^2+3m_K^2(p^2)}{w_K^4(p^2)}\Bigg)-[F'_{\pi NN}(p^2)]^2\Bigg], \tag{42}$$

$$\langle r^2\rangle^s_M=-\frac{9}{125}\left(\frac{g_A}{\pi F}\right)^2\int_0^\infty\frac{dp\,p^4}{w_K^3(p^2)}\Bigg[F^2_{\pi NN}(p^2)\Bigg(\frac{5}{16}R^2\mu_p^{LO}+\frac{p^2+3m_K^2(p^2)}{w_K^4(p^2)}\Bigg)+\frac{1}{2}[F'_{\pi NN}(p^2)]^2\Bigg], \tag{43}$$

where $F'_{\pi NN}(p^2)=dF_{\pi NN}(p^2)/dp$. In the analytical expressions the strange nucleon properties are related to the leading order nonstrange results of the charge radius of the proton $\langle r_E^2\rangle^P_{LO}$ of Eq. (13) and the proton magnetic moment μ_p^{LO} given by

$$\mu_p^{LO}=G_M^p(0)|^{LO}_{3q}=\frac{2m_N\rho R}{1+\frac{3}{2}\rho^2}. \tag{44}$$

Our results for the static characteristics of the nucleon associated with the vector current are listed in Table I. A comparison with other theoretical predictions is also included. For completeness, we also give our prediction for the leading strange charge coefficient ρ^s, which is defined as

$$\rho^s=\frac{dG_E^s(\tau)}{d\tau}\Big|\tau=(Q^2/4m_N^2)=0\,. \tag{45}$$

Note that ρ^s is also expected to be measured by the HAPPEX II experiment [36]. The two strange charge distribution parameters $\langle r^2\rangle^s_E$ and ρ^s are related in the PCQM as

$$\rho^s=-\frac{2}{3}m_N^2\langle r^2\rangle^s_E\,. \tag{46}$$

As we mentioned before, the error bars in our theoretical results are due to a variation of the range parameter R of the quark wave function from 0.55 fm to 0.65 fm. Also taking into account the other models, predictions cover a large range of values. In earlier calculations [7–10,13–17,19] the strange magnetic moment is favored to be negative, recent calculations [21,22], however, gave positive values for μ^s. Our value of μ^s is relatively small and negative, close to the one of Refs. [23,24]. Comparing our predicted values to HBChPT, though the central values of the quantities are quite different, the results are consistent if we take the error bars into account. For example, the strange magnetic moment and charge radius in the perturbative chiral quark model are -0.048 ± 0.012 and -0.011 ± 0.003 fm^2, and the corresponding values in HBChPT are 0.18 ± 0.34 and 0.05 ± 0.09 fm^2 [12]. For comparison, we also present the results generated by lattice QCD calculations: we indicate a calculation in the quenched approximation [9], which was recently

TABLE II. Predictions for SAMPLE, HAPPEX, and MAMI experiments in comparison to current experimental results.

Approach	$G^s_{\rm SAMPLE}(Q^2_{\rm S})$	$G^s_{\rm HAPPEX}(Q^2_{\rm H})$	$G^s_{\rm MAMI}(Q^2_{\rm M})$
HBChPT [12]	0.23 ± 0.44	0.023 ± 0.048	0.007 ± 0.127
χQSM [21]	0.09	0.087 ± 0.016	0.141 ± 0.033
CQM [24]	-0.06	-0.08	
PCQM	$-(3.7\pm 1.2)\times 10^{-2}$	$(1.8\pm 0.3)\times 10^{-3}$	$(2.9\pm 0.5)\times 10^{-4}$
Experiment [3,5]	$0.14\pm 0.29\pm 0.31$	$0.025\pm 0.020\pm 0.014$	

improved in Ref. [10], and one where the extrapolation scheme takes careful consideration of chiral symmetry constraints [8].

As for the leading strange charge coefficient ρ^s, the spread of predictions of various models is quite large, ranging from -2.93 to 3.06. Our value for ρ^s is positive and small: 0.17 ± 0.04. Our results for the strange radii are also small when compared to other approaches. Because of the simple relationship between ρ^s and the strange charge radius $\langle r^2\rangle^s_E$, a measurement of ρ^s also determines $\langle r^2\rangle^s_E$. A ^{4}He experiment was proposed to measure ρ^s at $Q^2\to 0$ to an accuracy of $\delta\rho^s=\pm 0.5$ which could be capable of yielding a reasonable experimental value for ρ^s [36]. In Ref. [36] the authors obtained a preliminary value of

$$\rho^s+2.9\mu^s=0.67\pm 0.41\pm 0.30 \tag{47}$$

from the current HAPPEX data [5]. In Table I we indicate our prediction for $\rho^s+\mu_p\mu^s$ of 0.05 at central values of ρ^s, μ_p and μ^s, which is consistent with Eq. (47). The values obtained from lattice calculations and the Skyrme model, where the strange magnetic moment is negative as in the PCQM, also compare reasonably to the value of Eq. (47). The results of dispersive approaches [13,14] and the NJL soliton model [20] disagree with the current experimental limits.

We also calculate the combinations of strange form factors measured by SAMPLE and HAPPEX at finite Q^2 with our predictions as: $G^s_{\rm SAMPLE}(Q^2_{\rm S})=-(3.7\pm 1.2)\times 10^{-2}$ and $G^s_{\rm HAPPEX}(Q^2_{\rm H})=(1.8\pm 0.3)\times 10^{-3}$. The prediction for the MAMI A4 experiment is $G^s_{\rm MAMI}(Q^2_{\rm M})=(2.9\pm 0.5)\times 10^{-4}$. In Table II we summarize the theoretical results for the respective experiments obtained within different theoretical approaches. The values of our predictions for the HAPPEX and MAMI experiments are quite small. This is because in the PCQM we have a cancellation between the strange charge form factor, which is positive and the magnetic one, which turns out to be negative, as will be shown below. In HBChPT, the central values of the SAMPLE and HAPPEX experiments are fitted by an appropriate choice of the low-energy couplings [12]. We also determine the strange axial charge of the nucleon with

$$g^s_A=-0.0052\pm 0.0015. \tag{48}$$

Our prediction has the correct sign when compared to the present direct estimate of this quantity from deep inelastic scattering experiments [37], $g^s_A=-0.12\pm 0.03$, but differs quantitatively.

Next we discuss the momentum dependence of the strange form factors for the central value of our size parameter $R=0.6$ fm. In Fig. 2 we plot the Q^2 dependence of the nucleon charge strange form factor, which is positive for all Q^2 and has maximum at $Q^2\sim 0.5$ GeV^2. The behavior of $G^s_E(Q^2)$ is close to the one calculated in Ref. [18] and similar to the results obtained in lattice QCD [9] and the chiral soliton quark model [21]. All these calculations give a positive strange form factor G^s_E. Our result is also consistent with that of Ref. [12] considering the uncertainty of the parameters. The chiral quark model of Ref. [24], however, obtains a form factor G^s_E which is negative and decreases with the increasing Q^2.

In Fig. 3, we show the momentum dependence of the strange magnetic form factor $G^s_M(Q^2)$ which is similar to the prediction of lattice QCD [9]. Both results give a negative strange form factor $G^s_M(Q^2)$. Though our results for G^s_E is

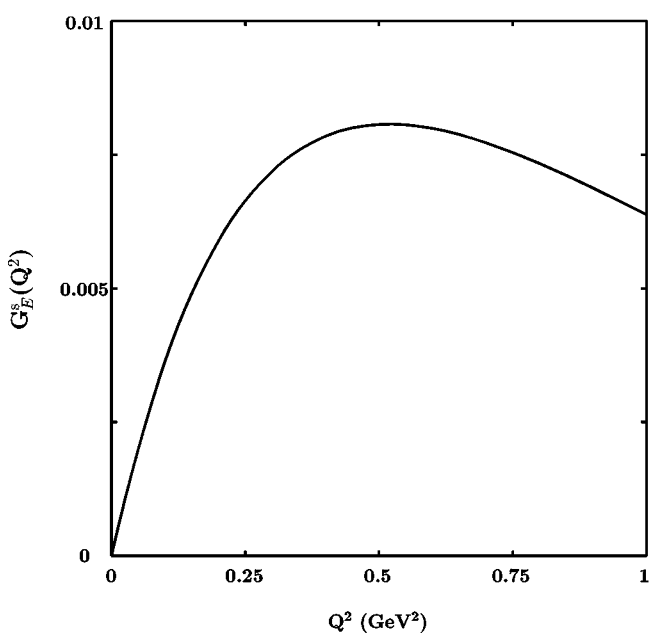

FIG. 2. Nucleon strange charge form factor $G^s_E(Q^2)$.

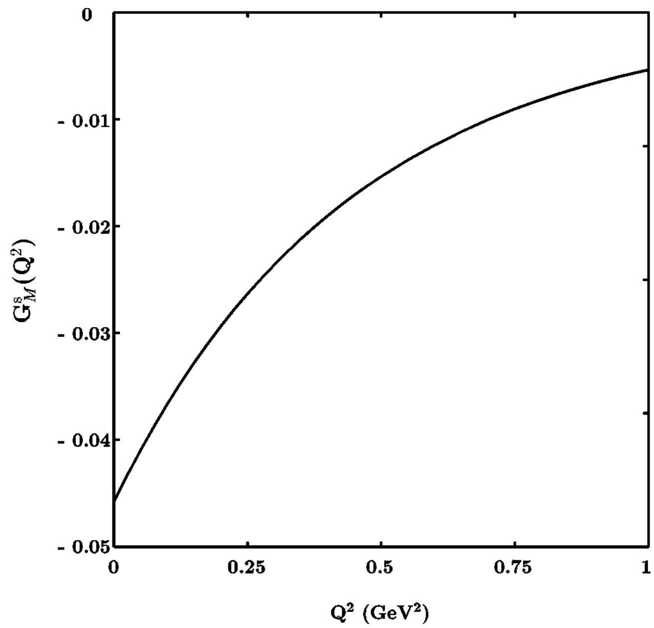

FIG. 3. Nucleon strange magnetic form factor $G_M^s(Q^2)$.

close to Refs. [18] and [21], the predictions for G_M^s are different, in that in latter references a positive value for G_M^s is obtained for the indicated Q^2 range. In Ref. [12], both positive and negative value of G_M^s are possible due to the uncertainty of the parameters.

In Figs. 4 and 5 we plot the momentum dependence of the Dirac $F_1^s(Q^2)$ and Pauli $F_2^s(Q^2)$ strange form factors of the nucleon. The behavior of F_1^s is close to that of G_E^s, while F_2^s and G_M^s have similar momentum dependence. Finally, in Fig. 6 we plot the Q^2-dependence of the normalized strange axial nucleon form factor $G_A^s(Q^2)/G_A^s(0)$.

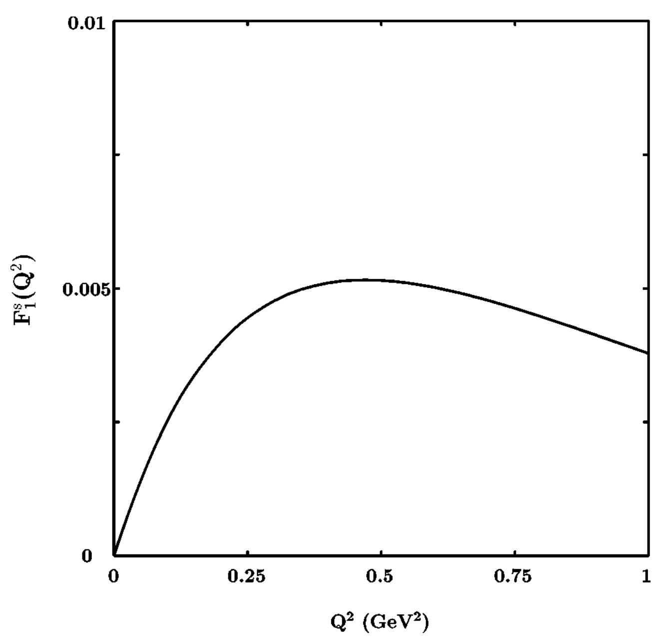

FIG. 4. Nucleon strange Dirac form factor $F_1^s(Q^2)$.

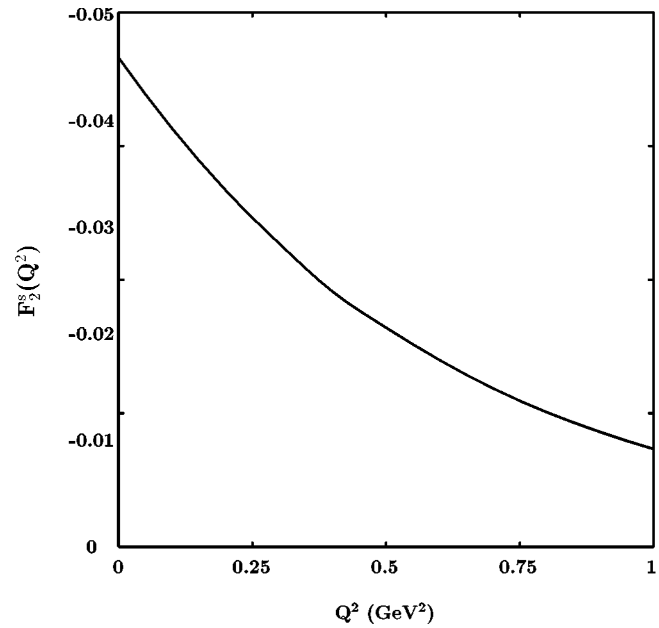

FIG. 5. Nucleon strange Pauli form factor $F_2^s(Q^2)$.

IV. SUMMARY

In summary, we investigate the strange vector (charge and magnetic) and axial form factors of the nucleon in the perturbative chiral quark model. We determined the momentum dependence of the strange form factors, radii, and magnetic moments at the one-loop level. Our results for the strange form factors and the leading strange charge coefficient are consistent with the SAMPLE and HAPPEX experiments. The strange electric form factor G_E^s is positive with a maximum at about $Q^2 \sim 0.5\ \mathrm{GeV}^2$. The strange magnetic form factor G_M^s is negative and its absolute value increases with

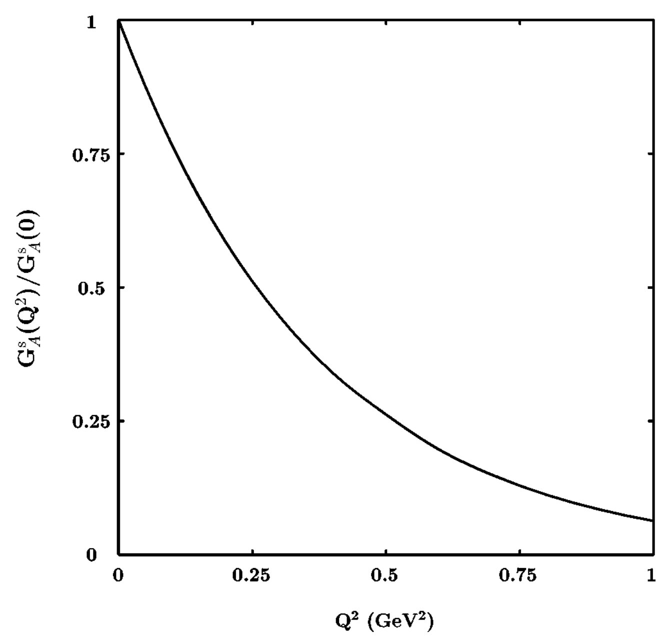

FIG. 6. Normalized nucleon strange axial form factor $G_A^s(Q^2)/G_A^s(0)$.

Q^2. The signs of the discussed quantities are stable with respect to changes in the model parameter. Absolute values for both G_E^s and G_M^s are small in this model, consistent with currently available data. An accurate determination of the strangeness form factors at moderate Q^2 will provide a sensitive test for the modeling of sea quark contributions in the low-energy description of the nucleon and hence for the implementation of chiral symmetry.

ACKNOWLEDGMENTS

P.W. would like to thank the Institute for Theoretical Physics, University of Tübingen for their hospitality. This work was supported by the Alexander von Humboldt Foundation and by the Deutsche Forschungsgemeinschaft (DFG) under Contract Nos. FA67/25-1 and GRK683.

[1] J. Ashman *et al.*, EMC Collaboration, Phys. Lett. B **206**, 364 (1988).
[2] B. Muller *et al.*, SAMPLE Collaboration, Phys. Rev. Lett. **78**, 3824 (1997).
[3] R. Hasty *et al.*, SAMPLE Collaboration, Science **290**, 2117 (2000).
[4] K.A. Aniol *et al.*, HAPPEX Collaboration, Phys. Lett. B **509**, 211 (2001).
[5] K.A. Aniol *et al.*, HAPPEX Collaboration, Phys. Rev. Lett. **82**, 1096 (2001).
[6] S. Köbis *et al.*, Nucl. Phys. B (Proc. Suppl.) **61**, 625 (1998).
[7] D.B. Leinweber, Phys. Rev. D **53**, 5115 (1996).
[8] D.B. Leinweber and A.W. Thomas, Phys. Rev. D **62**, 074505 (2000).
[9] S.J. Dong, K.F. Liu, and A.G. Williams, Phys. Rev. D **58**, 074504 (1998).
[10] N. Mathur and S.J. Dong, Nucl. Phys. B (Proc. Suppl.) **94**, 311 (2001).
[11] T.R. Hemmert, Ulf-G. Meissner, and S. Steininger, Phys. Lett. B **437**, 184 (1998).
[12] T.R. Hemmert, B. Kubis, and Ulf-G. Meissner, Phys. Rev. C **60**, 045501 (1999).
[13] R.L. Jaffe, Phys. Lett. B **229**, 275 (1989).
[14] H. Forkel, Phys. Rev. C **56**, 510 (1997).
[15] H.W. Hammer, Ulf-G. Meissner, and D. Drechsel, Phys. Lett. B **367**, 323 (1996).
[16] M.J. Musolf and M. Burkardt, Z. Phys. C **61**, 433 (1994).
[17] T.D. Cohen, H. Forkel, and M. Nielson, Phys. Lett. B **316**, 1 (1993).
[18] S. Dubnicka, A.Z. Dubnickova, and P. Weisenpacher, hep-ph/0102171.
[19] N.W. Park, J. Schechter, and H. Weigel, Phys. Rev. D **43**, 869 (1991).
[20] H. Weigel, A. Abada, R. Alkofer, and H. Reinhardt, Phys. Lett. B **353**, 20 (1995).
[21] A. Silva, H.C. Kim, and K. Goeke, Phys. Rev. D **65**, 014016 (2001).
[22] S.T. Hong, B.Y. Park, and D.P. Min, Phys. Lett. B **414**, 299 (1997).
[23] L. Hannelius, D.O. Riska, and L.Ya. Glozman, Nucl. Phys. **A665**, 353 (2000).
[24] L. Hannelius and D.O. Riska, Phys. Rev. C **62**, 045204 (2000).
[25] T. Gutsche and D. Robson, Phys. Lett. B **229**, 333 (1989); T. Gutsche, Ph.D. thesis, Florida State University, 1987.
[26] V.E. Lyubovitskij, T. Gutsche, and A. Faessler, Phys. Rev. C **64**, 065203 (2001).
[27] V.E. Lyubovitskij, T. Gutsche, A. Faessler, and E.G. Drukarev, Phys. Rev. D **63**, 054026 (2001).
[28] V.E. Lyubovitskij, Th. Gutsche, A. Faessler, and R. Vinh Mau, Phys. Lett. B **520**, 204 (2001); Phys. Rev. C **65**, 025202 (2002).
[29] S. Theberge, A.W. Thomas, and G.A. Miller, Phys. Rev. D **22**, 2838 (1980); **24**, 216 (1981).
[30] E. Oset, R. Tegen, and W. Weise, Nucl. Phys. **A426**, 456 (1984); R. Tegen, Ann. Phys. (N.Y.) **197**, 439 (1990).
[31] S.A. Chin, Nucl. Phys. **A382**, 355 (1982).
[32] J. Gasser, M.E. Sainio, and A.B. Svarc, Nucl. Phys. **B307**, 779 (1988).
[33] J. Gasser and H. Leutwyler, Phys. Rep. **87**, 77 (1982).
[34] D.H. Lu, A.W. Thomas, and A.G. Williams, Phys. Rev. C **57**, 2628 (1998).
[35] G.A. Miller and A.W. Thomas, Phys. Rev. C **56**, 2329 (1997).
[36] P. A. Souder *et al.*, Proposal to JLAB PAC 18, "Parity violation from ^{4}He at low Q^2: a clean measurement of ρ_s."
[37] W.M. Alberico, S.M. Bilenky, and C. Maieron, Phys. Rep. **358**, 227 (2002).